ELSEVIER

Materials Science and Engineering B 124–125 (2005) 261–265

MATERIALS SCIENCE & ENGINEERING B

www.elsevier.com/locate/mseb

Injection of point defects during annealing of low energy As implanted silicon

C. Tsamis [a,*], D. Skarlatos [a], V. Valamontes [b], D. Tsoukalas [c], G. BenAssayag [d], A. Claverie [d], W. Lerch [e]

[a] *IMEL/NCSR "Demokritos", 15310 Aghia Paraskevi, Athens, Greece*
[b] *Department of Electronics, Technological and Educational Institute of Athens, 122-10 Aegaleo, Greece*
[c] *Faculty of Applied Mathematical and Physical Sciences, National Technical University of Athens, 15780 Athens, Greece*
[d] *Toulouse Ion Implantation Group, CEMES/CNRS, 29 rue J.Marvig, 31055 Toulouse, France*
[e] *Mattson Thermal Products GmbH, Daimlerstr. 10, D-89160 Dornstadt, Germany*

Abstract

In this work, we investigate the interstitial injection into the silicon lattice due to high-dose, low energy arsenic implantation. The diffusion of the implanted arsenic as well as of boron, existing in buried δ-layers below the silicon surface, is monitored while successive amounts of the arsenic profile are removed by low temperature wet silicon etching. From the analysis of the diffusion profiles of both dopants, consistent values for the interstitial supersaturation ratio can be obtained. Moreover, the experimental results indicate that the contribution of the implantation damage to the TED of boron, and thus the interstitial injection, is not the main one. On the contrary, interstitial generation due to arsenic clustering seems to be more important for the present conditions.

Keywords: Injection; Point defects; Annealing

1. Introduction

One of the main issues in modern ULSI MOS devices is the reduction of the resistance of the source and drain junctions, which must be less than 10% of the channel resistance [1]. In order to achieve this, high-dose low energy arsenic implantation is used for the formation of ultra-shallow, highly doped junctions in the source/drain areas of the transistors. Arsenic is preferred to phosphorus due to its higher solid solubility limit and its lower diffusivity value. On the other hand, it is known that ion implantation leads to transient enhanced diffusion (TED) of dopants, a behaviour that is attributed to the damage induced by the implantation process. However, relatively to other dopants, such as boron and phosphorus, fewer studies have been performed for the TED of arsenic [2–6]. This is mainly because these effects are of moderate intensity at high temperatures and are more significant for very shallow junctions, less than 100 nm. In addition, research on arsenic is generally associated with high concentrations, where Fermi level dependence of dopant diffusion and point defects introduced by clustering or precipitation complicates the analysis of the implantation induced TED. In fact, there have been reported three sources for point defects that can contribute to the enhanced diffusion of arsenic and result in interstitial injection into the substrate. These sources are: (a) the end-of-range damage; (b) arsenic clustering; (c) arsenic precipitation. Moreover, as the implantation energy is reduced and the implanted profiles are moving closer to the surface, the influence of the surface would be more severe.

In this work, we investigate the origin of the TED and thus silicon interstitial injection caused by low energy, high-dose arsenic implantation. The approach consists in monitoring, at the same time, the diffusion of the implanted arsenic and of boron in buried δ-doped layers that exist below the silicon surface. Successive removal of the implanted silicon is performed, in order to control the total amount of damage, remaining in the silicon substrate, that will influence the buried boron layer. The etching process is performed at very low temperatures and it is not expected to influence the initial distribution of point defects,

* Corresponding author. Tel.: +30 2106503112; fax: +30 2106511723.
E-mail address: ctsamis@imel.demokritos.gr (C. Tsamis).

0921-5107/$ – see front matter © 2005 Elsevier B.V. All rights reserved.
doi:10.1016/j.mseb.2005.08.123

but will remove well-controlled depth slices from the damage profile.

2. Experimental procedure

2.1. Silicon etching at low temperatures

Various techniques, based on different types of solutions, have been reported in the literature for silicon etching at very low temperatures [7–9]. Celler et al. [7] have shown that by using a modified version of SC1 clean, 2.5–3 nm of silicon can be etched during the cleaning process. Schroer et al. [8] have used a 5% H_2O_2 solution at 75 °C to oxidize the surface, and subsequently, the native oxide was removed in a 3% HF solution. This technique has been successfully applied to controllably etch the silicon surface in B-doped samples, for TED experiments. In an alternative approach, Kasnavi et al. [9] used DI water for 30 min to etch around one monolayer of silicon. In this work, wet solutions based on H_2O_2 were evaluated at various temperatures (50–70 °C) for etching the silicon substrate.

The etching process consists of two steps:

(1) During the first step, the samples are immersed into the oxidizing solution, where an oxide is formed on the silicon surface. Since oxidation is taking place at room temperature, we do not expect to have any change of neither the boron nor the arsenic profile;
(2) During the second step, the samples are immersed in an HF solution, that dissolves the formed oxide. The combination of these two steps is referred to as "*one dip*".

During each cycle, an amount of silicon is removed from the substrate, this etched amount depending on the type and temperature of solution and the time of the immersion. In order to estimate the etching rate, parts of the surface of each sample were protected during the immersion by a thick oxide layer or an oxide/nitride bi-layer. Lines were lithographically patterned on the surface of the samples and the oxide or oxide/nitride bi-layer was etched inside the lines, so the silicon surface was exposed. Successive immersions were carried out in the two solutions (H_2O_2, HF). After the removal of the thick oxide layer, the initial silicon surface was revealed and served as reference for the measurements. The step height was measured by stylus profilometry and by atomic force microscopy (AFM). Fig. 1 is typical AFM image of the surface of the samples after the etching and the removal of all the protective layers. In addition to the step height, AFM was used to estimate the roughness of the etched surface as a function of the etching conditions. The average roughness of the silicon surface was in all cases less than 2 nm.

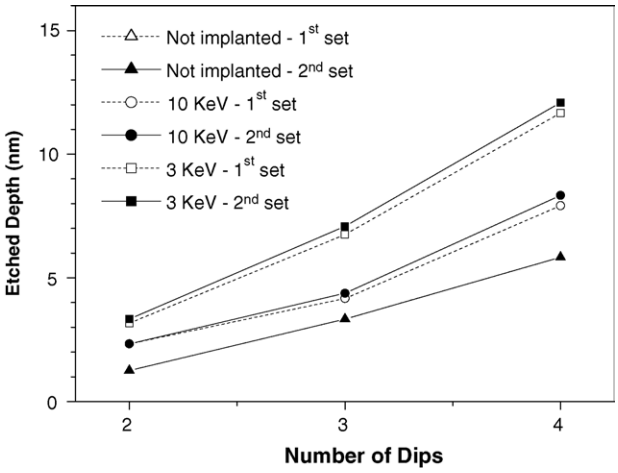

Fig. 2. Amount of removed silicon as a function of the number of dips in the solution and as a function of the implantation energy.

Fig. 2 shows the total amount of etched silicon as a function of the number of dips in 5% H_2O_2 solution at 50 °C, for a reference sample (not implanted) and for samples implanted with arsenic at 3 and 10 keV. We see that the implanted samples are etched in a faster rate compared to the reference sample, the rate being higher as the implantation energy decreases. In line with this observation, no significant difference in the etching process between implanted and un-implanted silicon samples was observed, when arsenic implantation was performed at higher energy (25 keV).

The reproducibly of the etching process was also examined in an alternative way. Two similar sets of samples were prepared consisting of various numbers of dips within the solution. The samples were implanted with arsenic at various energies (3, 10 and 25 keV) and doses (from 1×10^{15} to 2×10^{15} cm^{-2}). After the implantation, the wafers were cut in pieces and successive removal of the silicon surface was performed, in 5% H_2O_2 solution at 50 °C. The samples were, subsequently, RTA annealed at 950 °C for 30 s in N_2 ambient. SIMS analysis showed that the arsenic profiles of samples treated at the same conditions were almost identical, indicative of the good control of the etching process.

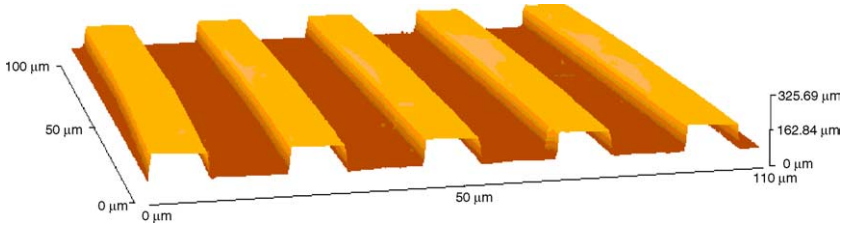

Fig. 1. Typical AFM image of the step formed on the silicon surface after the successive dips into the etching solutions and the removal of the protective layers. The average roughness of the silicon surface is less than 2 nm.

2.2. Study of interstitial injection

For the study of the interstitial injection, silicon wafers containing two boron δ-layers at depth of 0.6 and 1.1 μm, respectively, were used. The wafers were implanted with arsenic at 3 and 10 keV and a dose of 2×10^{15} cm^{-2}. The concentration of boron in δ-layers was of the order of 1×10^{18} cm^{-3}. Subsequently, etching of the silicon substrate was performed using 5% H_2O_2 solution at 50 °C. Various dips were performed in different samples, in order to locate the final silicon surface either before or after the position of the amorphous/crystalline interface. This is critical, since it represents the position of the extended defects band responsible for TED phenomena during amorphizing implants. For this purpose, cross-section TEM analysis was performed in order to estimate the depth of the amorphous region in each case. The depth of the amorphous region was 6 and 13 nm for the 3 and 10 keV implant, respectively, and was in good agreement with the predictions obtained by TRIM simulations. The samples were, subsequently, RTA annealed at 900 °C for two different times (5 and 30 s). As a final step, SIMS analysis was performed in order to estimate the boron and arsenic profile.

3. Results and discussion

SIMS profiling of very shallow implants can be challenging because a major fraction of the profile can fall within the surface transient of SIMS. For that reason, very carefully selected SIMS conditions must be applied. In a recent paper by Kasnavi et al. [10], it has been demonstrated that even when a 2 keV Cs primary ion beam is used, a significant portion of the shallow arsenic profile falls within the surface transient of the SIMS, resulting in an underestimation of the dose. The abruptness of SIMS is also limited. However, using a 750 eV Cs primary beam clearly improves the depth and abruptness resolution. Dosimetry can also be improved because the surface transient is reduced. Further reduction of the energy of the Cs beam results in marginal improvements and irregularities in the silicon signal are observed. These optimum conditions (750 eV Cs beam) were used for the analysis of the present samples, while a O_2 primary ion beam was used for boron profiling.

Fig. 3 shows the arsenic profiles for the samples implanted with As at 10 keV with dose 2×10^{15} cm^{-2} after RTA annealing in nitrogen for 30 s. From this figure, we notice that the arsenic dose that remains in the samples after the successive etching process decreases, in agreement to expected results. This is an indication that the etching process has been applied successfully. Fig. 4 shows the corresponding SIMS profile of the boron δ-layers for the same samples. From this figure, we notice that the broadening of the boron δ-layers is, with experimental error, independent of the etching process for all implantation energies. In addition, from the comparison between the SIMS profiles of the samples implanted with various energies, we can conclude that the broadening of the boron profile depends on the implantation energy and increases as the energy increases for the same annealing duration.

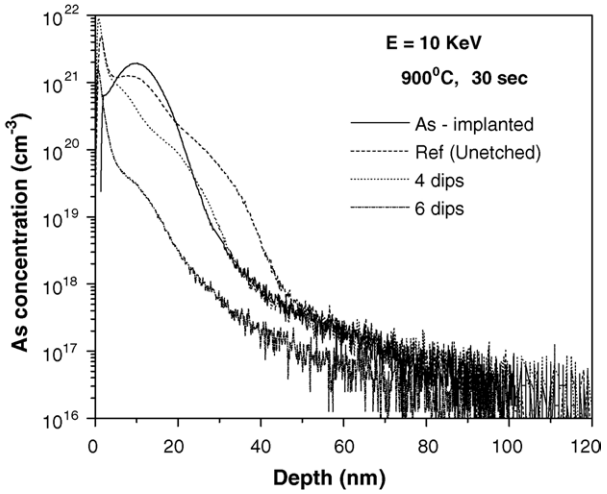

Fig. 3. Arsenic profile after silicon etching and RTA annealing at 900 °C for 30 s. The samples were implanted with arsenic at 10 keV with dose 2×10^{15} cm^{-2}.

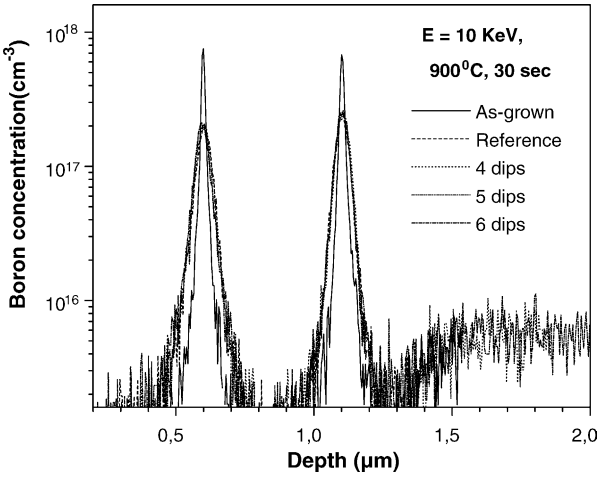

Fig. 4. Boron δ-layer profiles after the etching and annealing process at 900 °C for 30 s in samples implanted with arsenic at 10 keV with dose 2×10^{15} cm^{-2}.

In parallel, TEM analysis has been performed in order to investigate the existence of extended defects, after the annealing in the silicon substrate. Fig. 5 shows the silicon substrate in the case of 10 keV arsenic implantation, after RTA at 900 °C for

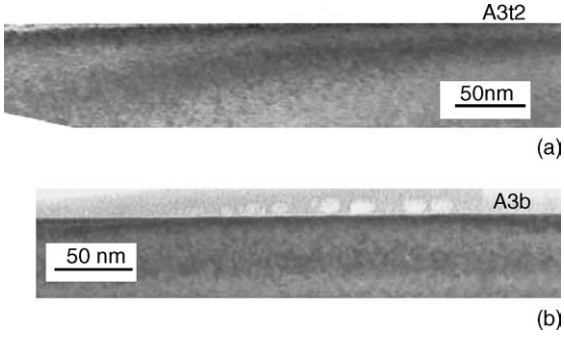

Fig. 5. Cross-section TEM images of: (a) reference sample (not-etched) and (b) after etching 15 nm of silicon, implanted with arsenic at 10 keV and dose of 2×10^{15} cm^{-2} and annealed at 900 °C for 30 s. We observe the full absence of extended defects.

30 s, for the reference (not-etched samples) and for the etched sample (after removing 15 nm of silicon). We observe the full absence of extended defects in both cases. This is probably due to the proximity of the surface, which acts as an interstitial sink absorbing the interstitials from the defects' band and leading to their dissolution. Similar results were also obtained for samples implanted with low energy (3 keV).

From the analysis of the boron and arsenic profiles, we can estimate the average supersaturation ratio of silicon interstitials for the current processing conditions. For this reason, FLOOPS software was used. It is generally accepted that dopant diffusion takes places via a dual mechanism, assisted by interstitials and vacancies. For boron, diffusion takes place predominantly by an interstitial mechanism. Under non-equilibrium conditions, the diffusivity enhancement of boron can be expressed as:

$$\langle D_B \rangle \approx f_B \frac{\langle C_I \rangle}{C_I^{eq}} D_B^{eq}$$

where C_I is the interstitial concentration, D_B the boron diffusivity, eq. denotes equilibrium and the parentheses $\langle\rangle$ denote time average. As a reference value for the equilibrium boron diffusivity, the expression $7.57 \exp(-2.46/kT)\,\mathrm{cm^2\,s^{-1}}$ was used and for the interstitial factor, we assumed $f_B = 1$.

In order to analyze the diffusivity enhancement of arsenic, we have followed an approach similar to the one described in a recent paper by Solmi et al. [11]. For the inert diffusion coefficient of arsenic, the default value of FLOOPS used for the constant diffusivity model was used, i.e.

$$D_{As} = D^x + \frac{n}{n_i} D^-,$$

where n is the electron concentration, n_i the intrinsic carrier concentration and D^x and D^- are the neutral and ionized diffusion coefficients, respectively, and are equal to $D^x = 12.04 \exp(-4.05/kT)\,\mathrm{cm^2\,s^{-1}}$ and $D^- = 6.66\mathrm{e}-2 \exp(-3.44/kT)\,\mathrm{cm^2\,s^{-1}}$. By assuming that the interstitial supersaturation that supports TED increases the neutral term of the diffusion coefficient D^x by a factor a_x, the TED diffusivity of arsenic can be described as

$$D_{As}\,(\mathrm{TED}) = a_x D^x + \frac{n}{n_i} D^-$$

The diffusivity enhancement for low arsenic concentrations, as in the tail region, can be estimated by the ratio D_{As}/D_{As} (TED), assuming $n = n_i$. Taking into account that the interstitial factor for arsenic diffusion is $f_{As} = 0.5$, the interstitial supersaturation in this case is twice the value estimated for the diffusivity enhancement.

Fig. 6 shows the supersaturation ratio of silicon interstitials, as a function of the position of each boron δ-layer and at the surface, for the two different arsenic implantation conditions after annealing at 900 °C for 30 s. It is important to note that consistent results for the interstitial supersaturation were obtained from the analysis of the profiles

In order to have a more clear idea of the obtained results, it is useful to discuss about the various mechanisms that influence point defect kinetics in the case of low energy implanted silicon. It is accepted that the transient enhanced diffusion is due

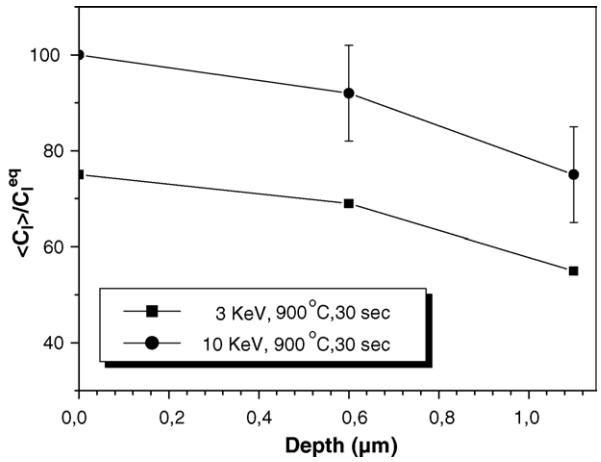

Fig. 6. Estimation of interstitial supersaturation as a function of the position of each boron δ-layer and at the silicon surface, due to arsenic implantation and annealing.

to the interstitial supersaturation induced by the implantation damage. An interstitial supersaturation is maintained during the Ostwald ripening process that is taking place during the formation and evolution of the extended defects, as these evolve from ⟨3 1 1⟩ defect to dislocation loops. When the band of the defects is located away from the surface (at a distance much larger than the mean radius of the loop distribution), the ripening process is conservative and the number of bounded interstitials within the loops remains almost constant. This number represents the recoiled interstitials survived the recombination with vacancies at the crystalline part. This is the part of the implantation damage responsible for anomalous dopant diffusion. However, when the surface is very close to the defect band, the ripening process is non-conservative since the surface is a strong sink for interstitials.

According to that, we expect that decreasing the distance between the defect band and the surface (by removing silicon) would lead to a reduction of the interstitial supersaturation within the defect band (due to more effective interstitial loss), and consequently, to reduction of the enhanced diffusion of boron δ-layers. This is expected to be more evident in the case where the etched depth was more than the thickness of the amorphous layer. However, as we can notice from the comparison between the reference sample (not-etched) and the samples that were etched at the surface, no significant differences in the diffusion of the boron profile were observed. This indicates that the TED of boron is not only due to the supersaturation maintained during defect evolution. In fact, there is a strong possibility that in the case of low energy implants, all the defects might have dissolved This is supported by the TEM analysis that showed the absence of dislocation loops in the sample after annealing at 900 °C for 30 s. In fact, it has been recently reported in the literature that no defect survived after a 5 keV, $10^{15}\,\mathrm{cm^{-2}}$ As implantation after annealing at 850 °C for 10 s [12].

However, there are two more sources for point defects, especially in the case of high arsenic concentration. When the arsenic concentration exceeds the solid solubility of arsenic in silicon, arsenic clustering may occur. Electrical activation studies

have attributed arsenic clusters to be the cause of dopant deactivation in silicon [13]. These studies have also determined a critical concentration for arsenic cluster formation, which is a function of the annealing temperature. Theoretical studies and experimental evidence indicate that arsenic clusters form around a vacancy with the consequent injection of silicon interstitials. The proposed mechanism can be described by the reaction:

$$n\mathrm{As} \Leftrightarrow \mathrm{As}_n V + I$$

where n assumes values between 2 and 4.

In a recent work, Solmi et al. [11] estimated that about one-third of the TED observed in the first 20 min of annealing is due to the defects produced by clustering. It is very probable that this is the main mechanism that is responsible for TED in our experimental conditions.

Another possible mechanism that might influence defect kinetics is As precipitation. It has been reported that extended defects at the projected range are absent when the arsenic concentration approaches the critical value for precipitation. This is probably due to vacancies released during SiAs precipitation leading to the annihilation for extended defects. However, the formation of SiAs precipitates is not very probable in our experimental conditions due to the very high values of the solid solubility of arsenic in Si and the difficulty of nucleation of this conjugate phase.

4. Conclusions

In this work, we have investigated the damage generated by low energy, high-dose arsenic implantation performed at room temperature and the subsequent interstitial injection into the substrate. The diffusion of the arsenic profile, as well as the diffusion of boron buried δ-doped was monitored and the supersaturation ratio of silicon interstitials was estimated in a consistent manner after the analysis of the results for both dopants. Information about the mechanism that contributes mainly to silicon interstitial injection under these conditions was presented.

Acknowledgments

The authors acknowledge Prof. Stoemenos (University of Thessaloniki) for performing the TEM analysis, Philips for providing the wafers with the boron δ-layers and ISE (now Synopsys) for providing FLOOPS software. This work was supported by the EU through the IST Project No. 2000-30129 FRENDTECH “Front-End Models for Future Technology”.

References

[1] J.D. Plummer, M.D. Deal, P.B. Griffin, Silicon VLSI Technology, first ed., Prentice Hall Electronics and VLSI Series, 2000, p. 373.
[2] Y. Kim, H.Z. Massoud, R.B. Fair, J. Electron. Mater. 18 (1989) 143.
[3] V. Krishnamoorthy, B. Beaudet, K.S. Jones, D. Venables, Tech. Dig. Int. Electron Devices Meet. (1997) 638.
[4] V. Krishnamoorthy, K. Moller, K.S. Jones, D. Venables, J. Jackson, L. Rubin, J. Appl. Phys. 84 (1998) 5997.
[5] K.S. Jones, D. Downey, H. Miller, J. Chow, J. Chen, M. Puga-Lambers, K. Moller, M. Wright, E. Heitman, J. Glasberg, M. Law, L. Robertson, R. Brindos, Tech. Dig Int. Electron Devices Meet. (1999) 841.
[6] R. Kim, T. Aoki, Y. Furuta, H. Kobyashi, J. Xia, T. Saito, Y. Kamakura, K. Taniguchi, Mater. Res. Soc. Symp. Proc. 610 (2000) B8.2.1.
[7] G.K. Celler, D.L. Barr, J.M. Rosamilia, Electrochem. Solid-State Lett. 3 (1) (2000) 47–49.
[8] E. Schroer, V. Privitera, F. Priolo, E. Napolitani, A. Camera, Appl. Phys. Lett. 76 (21) (2000) 3058.
[9] R. Kasnavi, Y. Sun, R. Mo, P. Pianetta, P.B. Griffin, J. Plummer, J. Appl. Phys. 87 (5) (2000) 2255.
[10] R. Kasnavi, Y. Sun, G. Mount, P. Pianetta, P.B. Griffin, J. Plummer, Electrochem. Solid-State Lett. 4 (1) (2001) G1–G3.
[11] S. Solmi, M. Ferri, M. Bersani, D. Giubertoni, V. Soncini, J. Appl. Phys. 94 (4) (2003) 4950.
[12] D. Girginoudi, N. Georgoulas, A. Thanailakis, E.K. Polychroniadis, E-MRS Spring Meeting, Symposia Proceedings 159, Strasburg, 2004, p. 381.
[13] S. Whelan, V. Privitera, G. Mannino, M. Italia, C. Bongiorno, A. La Magna, E. Napolitani, J. Appl. Phys. 90 (8) (1998) 5997.